Static Fiber-Bragg Grating Strain Sensing Using Frequency-Locked Lasers

Ady Arie, *Senior Member, IEEE, Member, OSA,* Boaz Lissak, and Moshe Tur, *Fellow, IEEE, Fellow, OSA*

***Abstract*—Novel and highly sensitive static strain interrogation technique is demonstrated, where the sensing element is a fiber-Bragg grating (FBG) and the light source is a frequency-locked diode laser. Locking the laser frequency to the center of an absorption line (atomic line of potassium in our experiment) eliminates the slow frequency drift of the laser. The stabilized laser source is used to measure low frequency ("static") strain, with a sensitivity of 1.2 nanostrain/$\sqrt{\text{Hz}}$ rms at 1.5 Hz.**

***Index Terms*—Gratings, optical fiber devices, strain measurement.**

I. Introduction

DUE to their fiber-based, wavelength encoded operation, fiber Bragg gratings (FBG's) offer attractive sensing possibilities, especially in strain and temperature embedded sensing of smart structures [1]. The small physical dimensions of the FBG enables localized sensing at the position of the FBG. Furthermore, multiplexed sensing is possible by using several different FBG's on the same strand of optical fiber. Strain measurements can be subdivided into low frequency measurements ($\leq$10 Hz), often called "static" measurements and higher frequency measurements, usually termed "dynamic" measurements. Typical sensitivities of FBG strain sensors are in the range of 1 microstrain/$\sqrt{\text{Hz}}$ rms [1]. To the best of our knowledge the highest static strain sensitivity for an FBG-based sensor [2], having a resolution of 6 nanostrain/$\sqrt{\text{Hz}}$, was obtained by using an isolated reference FBG and interferometric wavelength shift detection. As for dynamic strain measurements, very high sensitivities were obtained using interferometric wavelength shift detection scheme [3], [4] or special π-shifted FBG [5].

In this paper we present a novel, passive and narrowband interrogation technique for both *static* and *dynamic* FBG strain measurements, capable of very high sensitivity and high resolution. The measured sensitivity is comparable with the best results obtained using a single FBG sensor. In our method, a single longitudinal mode laser is used to probe the wavelength shift in the reflection curve of an FBG imposed by a strain or temperature signal. Consider the case where the midreflection frequency of the FBG coincides with the laser frequency. A strain or temperature change will shift the reflection curve of the FBG, hence the reflected power from the grating will vary with proportion to the applied change. However, the slow frequency drifts of the interrogating laser may also be interpreted as a false signal. By locking the laser frequency to an atomic or molecular absorption line, these frequency drifts may be practically eliminated [6]. In this case, the static strain or temperature signal can be derived from the low frequency or dc photocurrent of the reflected signal.

When restricted to dynamic strain measurements, the method can be significantly simplified, as we have already described in a recent letter [7]. In this case, rather than locking to an atomic line, the laser is locked directly to the midreflection frequency of the FBG using a low-frequency servo, thereby stabilizing the operating point against slow strain and temperature drifts, as well as frequency drifts of the interrogating laser. The laser wavelength will not track dynamic strain variations at frequencies above the unity gain frequency of the servo. The dynamic strain at those frequencies can thus be directly derived from the ac photocurrent of the reflected signal. Using this scheme we have obtained high strain sensitivity of 45 picostrain/$\sqrt{\text{Hz}}$ rms at 3 kHz with a measured dynamic range of 110 dB [7].

A theoretical model of the frequency-locked FBG sensor, its noise sources and expected sensitivities are presented in Section II. Experimental static strain measurements are presented in Sections III, and the results are summarized in Section IV.

II. Theoretical Modeling

A. Method of Operation

Assuming a linearized reflection slope of the FBG, the reflection coefficient, R_f, of the free, unstrained FBG around the midreflection point can be modeled as (see Fig. 1)

$$R_f(\nu) = R_0 + G \cdot (\nu - \nu_0) \tag{1}$$

where ν is the optical frequency, G is the grating reflectivity slope and ν_0 and $R_0(= R_f(\nu_0))$ are, respectively, the midreflection frequency and reflection coefficient of the unstrained fiber. An applied strain, ε will shift the FBG reflection curve by $\Delta\nu_s$, which we experimentally determined to obey $\Delta\nu_s/\nu = -0.79\varepsilon$ [1]. The reflection curve of the strained fiber, therefore, becomes $R_f(\nu - \Delta\nu_s)$. When an input light with a power level of P_0 is sent toward the grating, the reflected signal generates at PD1 a photocurrent

Manuscript received December 28, 1998; revised July 9, 1999. This work was supported in part by the Israeli Ministry of Science and Technology, by the Maria Rossi Ascoli Foundation, and by the U.S.–Israel Binational Science Foundation under Grant 94-301.

The authors are with the Faculty of Engineering, Tel-Aviv University, Tel-Aviv 69978 Israel.

Publisher Item Identifier S 0733-8724(99)08007-X.

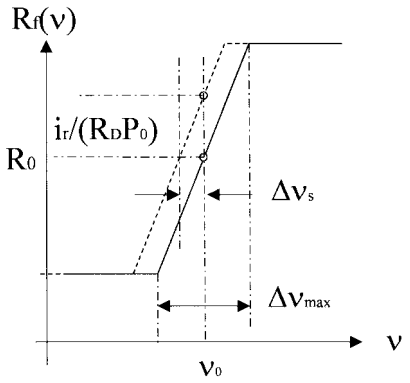

Fig. 1. The effect of applied strain on the FBG reflectivity curve. Solid and dashed lines represent the unstrained and strained FBG reflectivity curves, respectively.

of $I_r(\nu) = R_f(\nu - \Delta\nu_s)R_D P_0$, where R_D is the detector responsivity.

If the laser frequency is locked to a stable frequency reference, the static strain can be derived directly from the DC (or low frequency) photocurrent of the signal reflected form the FBG. Possible frequency references include another isolated FBG [2], an interferometric reference—e.g., a Fabry–Perot cavity [8], or an atomic or molecular transition. The highest long-term stability and accuracy is achieved by locking to atomic/molecular references. These absorption lines are very stable with respect to the operating conditions. For example, semiconductor lasers locked to Rb Doppler-broadened lines have negligible temperature induced frequency shifts ($\ll$1 MHz/°C) and very small intensity induced shift ($-$5 MHz/(mW/cm^2) [6]. For comparison, the center reflection frequency of an FBG has a temperature-induced frequency shift of $-$1.2 GHz/°C [1]. Even a thermally compensated FBG has a typical shift of $\approx$ 50 MHz/°C [9]—much larger than that of atomic or molecular lines. Thus, it appears that frequency-locking of the interrogating laser (at around 1550 nm) to atomic or molecular absorption lines should make it possible to reduce the laser frequency drift to the sub-MHz level.

Absorbers in the 1550 nm wavelength range include several molecular lines, e.g., NH_3, C_2H_2, HCN, HI [10], as well as excited states of atomic lines e.g., Kr [11] or Rb [12]. Another option is to double the laser frequency and lock to absorbers in the second harmonic, for example the Rb D2 line at 780.25 nm [13], [14] or the potassium (K) D_1 line at 770.109 nm [15], [16]. We chose to lock the laser to the potassium D_1 line. The advantage of this transition is that its Doppler-broadened spectrum is very simple—it has only a single Doppler broadened line in the relevant wavelength range, hence the frequency identification is very easy.

For dynamic strain measurements, the laser frequency is locked to the midreflection frequency of the FBG [7]. This can be considered as a special case in which the frequency reference is the FBG sensing element itself. In this case, the dc photocurrent is maintained at $R_0 R_D P_0$ even in the presence of a slowly varying strain or temperature. A dynamic strain at a frequency exceeding the unity gain frequency of the servo will generate an ac photocurrent that is proportional to the dynamic strain. In the method presented here, the laser is locked to the center of an atomic line. An applied strain shifts the reflection curve $\Delta\nu_s$, thus altering the reflection coefficient by $-G\Delta\nu_s$ and the dc photocurrent by

$$i_r = -GR_D P_0 \cdot \Delta\nu_s = [0.79\nu G R_D P_0]\varepsilon \tag{2}$$

from which the strain is easily determined. Dynamic strain measurements are also possible when the laser is locked to an atomic or molecular line. In this case, however, the operating point may differ from the midreflection frequency of the FBG.

B. Sensitivity Limits

Unlike other interrogation architectures that use broadband sources [3], our narrowband technique can provide the detector with high enough optical power so that all detector noise contributions are negligible. The sensitivity limits of this sensing technique are set by the laser shot and intensity noise, the spontaneous emission induced frequency noise of the laser, as well as the temperature-induced refractive index fluctuations of the FBG itself.

The shot noise, being a fundamental type of noise, always accompanies the average photocurrent $R_0 R_D P_0$ (assuming for simplicity that the atomic transition is near the midreflection frequency of the FBG) and its standard deviation is $i_s = \sqrt{2eR_0 R_D P_0 B}$ where e is the electron charge and B is the detection bandwidth. Using (2), the minimum detectable strain imposed by shot noise is

$$\varepsilon_{\min(\text{shot})} = (0.79\nu G)^{-1}\sqrt{\frac{2eR_0 B}{R_d P_0}}. \tag{3}$$

If $R_0 = 0.5$, $R_D = 1$ Amp/Watt, $P_0 = 100$ μW, $B = 1$ Hz, $G = [35\text{ GHz}]^{-1}$ and $\nu = 195$ THz ($\lambda = 1540$ nm), the minimum detectable strain is $\varepsilon_{\min(\text{shot})} = 9{\cdot}10^{-12}/\sqrt{\text{Hz}}$. The laser intensity noise should be also considered. For a given Relative Intensity Noise (RIN) $\equiv 20\log(\Delta P_{(\text{int. noise in 1 Hz band})}/P_0)$ [dB/Hz]), one gets from (2)

$$\varepsilon_{\min(\text{RIN})} = \frac{10^{\text{RIN}/20}R_0 R_D P_0\sqrt{B}}{0.79\nu G R_D P_0} = \frac{10^{\text{RIN}/20}R_0\sqrt{B}}{0.79\nu G}. \tag{4}$$

For a fairly low noise laser with a RIN of $-$145 dB/Hz the minimum detectable strain becomes $\varepsilon_{\min(\text{RIN})} = 6{\cdot}10^{-12}/\sqrt{\text{Hz}}$.

The second fundamental limitation is the spontaneous-emission-induced frequency noise of the laser. In an ideal laser, only the spontaneous emission process contributes to the laser frequency noise. In this case, the laser lineshape is Lorentzian with a linewidth $\Delta\nu_L$, and the frequency noise power spectral density is $S_f = \Delta\nu_L/\pi$, in units of Hz^2/Hz [17]. In a bandwidth of B Hertz the standard deviation of this frequency noise is $\sqrt{S_f B}$. Obviously, this frequency noise, which is interpreted by the FBG as strain noise, will set the following limit to the sensor sensitivity:

$$\varepsilon_{\min(\text{frequency})} = \frac{\sqrt{S_f B}}{0.79\nu}. \tag{5}$$

For a typical tunable external cavity semiconductor laser $\Delta\nu_L = 1$ MHz, $\sqrt{S_f} = 560$ Hz/$\sqrt{\text{Hz}}$, $\varepsilon_{\min(\text{frequency})} = 3.6 \cdot 10^{-12}/\sqrt{\text{Hz}}$. In practice, the frequency noise spectral density is often higher than the level induced by spontaneous emission, due to technical noises caused, for example, by acoustic and thermal disturbances. Depending on the frequency noise level, the sensitivity may be limited either by the frequency noise or by the shot noise.

If there are parasitic reflections, e.g., from various fiber ends or from connectors, they may create ghost interferometers. The interferometric signal will fluctuate, owing to the laser frequency noise and to small variations in the optical path length, thus limiting the sensor sensitivity and accuracy. Consider for example that two signals, from the FBG and from a parasitic reflector with an effective reflectivity of R_p, are reaching the detector. The interferometric current noise under a worst case condition in which the two signals have the same polarization is $2R_D P_0 \sqrt{R_p R_0}\cos(\Delta\varphi)$, where $\Delta\varphi = 2\pi(\nu + \delta\nu)\tau$ and τ are the phase difference and the delay between the two signals, respectively, and $\delta\nu$ is the instantaneous laser frequency deviation. The highest noise level is obtained in the quadrature points of the interferometer [18], i.e., when $2\pi\nu\tau = \pi/2 + m\pi$. In this case, the standard deviation of the interferometric current noise for a detection bandwidth B much smaller than $1/\tau$ is $4\pi R_D P_0 \tau \sqrt{R_p R_0 S_f B}$. This current noise will be interpreted by the sensor as strain noise, thus imposing a minimum detectable strain of

$$\varepsilon_{\min(pn)} = \frac{4\pi\tau\sqrt{R_p R_0 S_f B}}{0.79\nu G}. \tag{6}$$

Assuming that the parasitic reflectance is 10^{-6} and the delay between the two signals is 3.3 ns (accumulated in 1 m of fiber), the minimum detectable strain is $\varepsilon_{\min(pn)} = 3.76 \cdot 10^{-12}/\sqrt{\text{Hz}}$. In addition, slow variations in the average phase term $2\pi\nu\tau$ may cause errors in determining the static strain. The effects of these variations can be averaged to zero by dithering the fiber length using a piezo-electric transducer (thus changing the relative delay τ) or the laser frequency ν at a rate higher than the detection bandwidth of the sensor.

Another fundamental noise contribution is due to thermally induced refractive index fluctuations [19], which cause a beam propagating through the fiber to accumulate a phase error on the order of 1 μRad/$\sqrt{\text{Km} \cdot \text{Hz}}$ (at room temperature). Translating this figure to the thermally induced frequency fluctuations of the FBG reflection curve, one obtains for a 1 cm long FBG a strain sensitivity limit of $\varepsilon_{\min(\text{thermal})} < 10^{-13}/\sqrt{\text{Hz}}$, which is negligible with respect to the shot noise and laser frequency noise.

Another effect that may practically limit the performance of the sensor is the sensitivity to dynamic perturbations in the fiber leads. These perturbations may change the power level reaching the detector, thus may be falsely interpreted as strain changes in the system. Various schemes can be used to eliminate the sensitivity to perturbations in the fiber leads. For example, variations in the transmission of the fiber leads can be measured independently by using another reference FBG placed near the sensing FBG and a light source at a different wavelength.

C. Dynamic Range

The linear dynamic range of the measurable strain is determined by the spectral width, $\Delta\nu_{\max}$, of the linear section in the FBG reflectivity curve, see Fig. 1. Thus, the highest peak to peak measurable dynamic strain becomes $\varepsilon_{\max} = \Delta\nu_{\max}/0.79\nu$. To achieve a larger $\varepsilon_{\max}$ one should increase $\Delta\nu_{\max}$, which is equivalent to reducing the reflectivity versus wavelength slope. It will also increase the shot noise and intensity noise contributions, but will have no effect on the frequency noise contribution. Hence, if the system is limited by frequency noise, it is worthwhile to increase $\Delta\nu_{\max}$ up to a critical value at which the shot noise contribution becomes equal to the frequency noise contribution. This will increase the dynamic range without reducing the sensitivity. By comparing the sensitivity limits imposed by the frequency noise to that of the shot noise, using $G = 2R_0/\Delta\nu_{\max}$ and (3) and (5), the critical $\Delta\nu_{\max}$ is given by:

$$\Delta\nu_{\max,\text{critical}} = \sqrt{2R_0 R_D P_0 S_f / e}. \tag{7}$$

Using the values given above, $\Delta\nu_{\max,\text{critical}} = 14$ GHz and $\varepsilon_{\max} = 90$ microstrain peak to peak. With a proper design of the FBG—e.g., by using a very short FBG or a chirped and strongly apodized grating with asymmetric reflectivity profile [20], [21]—the dynamic range can be increased as desired but at the expense of sensitivity and resolution. FBG with a moderate and asymmetric reflection slope having a bandwidth exceeding 15 nm are now commercially available [9], thus enabling strain measurements up to a limit determined by the tensile strength of the FBG. As an example, assuming a dynamic range of 5000 microstrain, the FBG slope will be $G = [770\ \text{GHz}]^{-1}$, and the shot noise limited sensitivity, according to (3), is $2 \cdot 10^{-10}/\sqrt{\text{Hz}}$, which is still substantially better than the typical FBG sensors performance.

III. Static Strain Measurements

We have constructed the FBG static strain sensor, shown in Fig. 2 and experimentally tested its performance. The tunable laser source, New Focus model 6262, is coupled into a 3-cm long periodically poled LiNbO3 waveguide frequency doubler [22]. The pump and frequency-doubled beams were separated using a dichroic beams-splitter. The pump beam was coupled into the sensing optical fiber. The FBG reflection, centered at 1540 nm with a peak reflection of $\geq$96%, had fullwidth at half-maximum (FWHM) of 1.5 nm and a linear width of $\Delta\nu = 35$ GHz. The fiber could be strained using a piezo-electric actuated mount. To eliminate parasitic interference between the FBG and all fiber terminations, we used angled connectors (APC) and tightly bent the unused fiber ports. The second harmonic signal with a power of ≈ 1 μW was generated in the waveguide doubler and sent into a 10-cm long potassium absorption cell. The cell was heated to a temperature of 35°C in order to increase the vapor pressure (and thus the absorption). The absorption signal, shown in the inset of Fig. 3, was obtained by taking the difference between two Si detectors—one measured the transmitted power through the absorption cell while the other probed the input power into

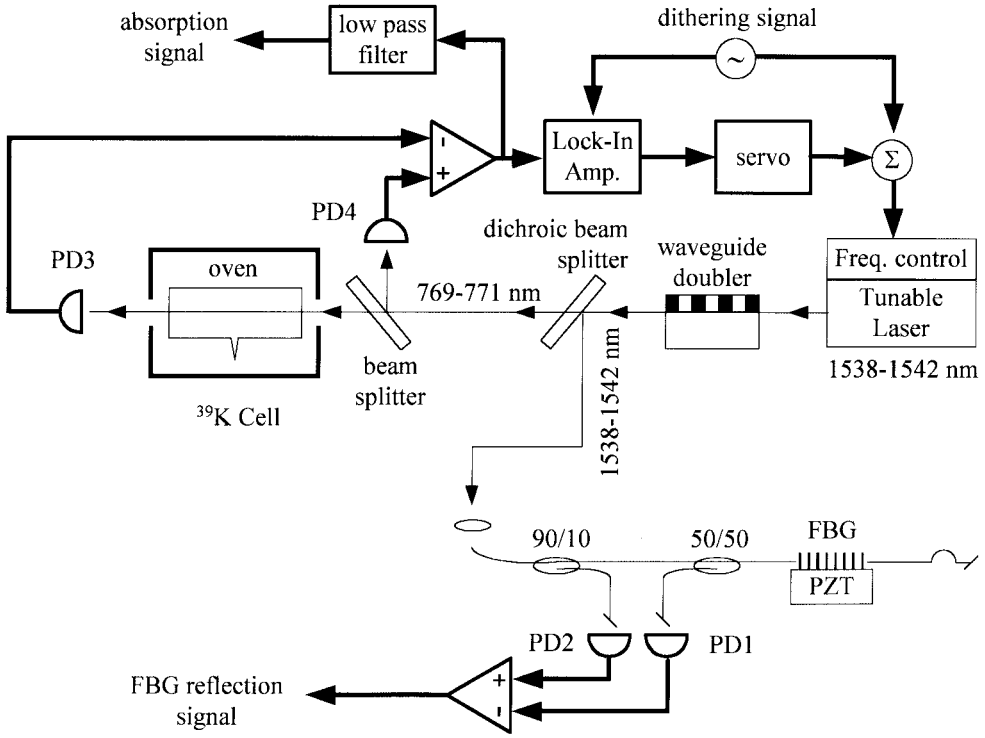

Fig. 2. Static strain measurement setup. PD1 and PD2 are InGaAs photodetectors. PD3 and PD4 are Si photodetectors.

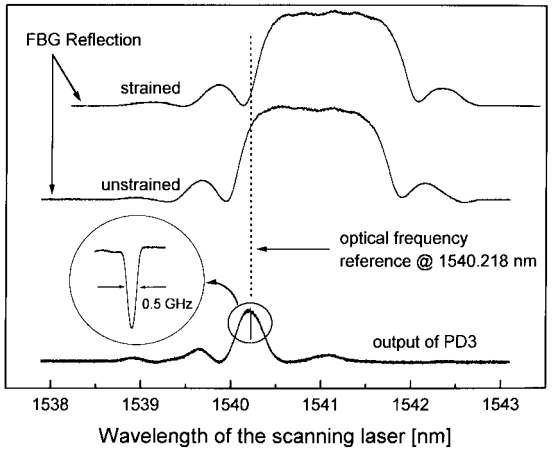

Fig. 3. Reflection curve of the FBG with two different strain levels, and the transmitted second harmonic power through the absorption cell (PD3), as function of the scanning laser wavelength. The sharp dip in the second harmonic power is the potassium absorption line @ 770.109 nm (obtained when the laser wavelength is 1540.218 nm). The inset shows an expanded scan of the potassium absorption line.

the cell. The absorption line we observed included several transitions between the atomic levels $4S_{1/2} \rightarrow 4P_{1/2}$ of ^{39}K [23], but they could not be resolved owing to the Doppler-broadening ($\approx$ 770 MHz at room temperature). The obtained linewidth is $\approx$ 1 GHz at 770 nm, which provides a frequency marker having a width of $\approx$ 500 MHz near 1540 nm.

The potassium absorption line provided a stable frequency reference. Fig. 3 also shows a scan of the FBG reflection profile. When the fiber is strained, the FBG reflection curve is shifted toward longer wavelengths. However, when static measurements are made without accurate wavelength monitoring, similar shifts can result not from strain but from frequency drifts of the scanning laser. Hence, if the laser is locked to the center of the almost temperature-independent potassium absorption line, all measured shifts can be exclusively attributed to the effects of strain and/or temperature on the fiber grating.

Wavelength-modulation spectroscopy was used to obtain a derivative signal of the absorption line: The laser frequency was modulated using a built-in PZT-frequency control actuator at a frequency of 1 kHz and a modulation depth of 900 MHz. This absorption signal was demodulated using a lock-in amplifier (LIA) and was used as an error signal for locking the laser to the center of the line. It was fed through a servo amplifier back into the PZT frequency control actuator of the laser. The open loop gain of the locking system as a function of the frequency f in Hz was $\approx 500/f$. Averaging over a frequency range of 900 MHz also helped in smoothing any parasitic roughness of the linear part of the $R_f(\nu)$ function [see (1)]. In any case, as long as $R_f(\nu)$ is monotonic in ν, any deviations from a linear slope can be handled by proper calibration.

We have characterized the response and sensitivity of this strain sensor in the time domain, Fig. 4 and in the frequency domain, Fig. 5. We have applied a series of voltage steps to the PZT, which strained the fiber by successive strain increments of 2.3 $\mu\varepsilon$. As expected, the reflection signal followed these voltage steps, see Fig. 4. The strain noise spectral density was measured using a fast Fourier transform (FFT) spectrum analyzer. A 0.23-μstrain rms calibration signal at 1.5 Hz was applied to the PZT-actuated fiber holder. The measured signal to noise ratio was 63 dB with a resolution bandwidth of 18.7 mHz, hence the static strain sensitivity was 1.2 nanostrain/$\sqrt{\text{Hz}}$, see Fig. 5. The limiting noise in this case was the environmental acoustic noise.

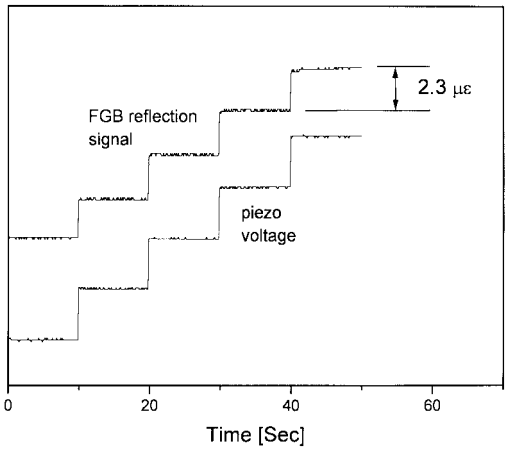

Fig. 4. Time traces showing a series of voltage steps applied to a PZT-controlled fiber holder, which strained the FBG, together with the reflection signal from the FBG, measured using the setup shown in Fig. 2.

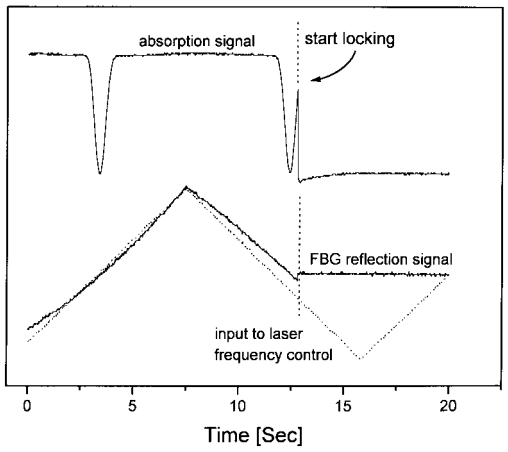

Fig. 6. The effect of triangular-shaped variation of the laser frequency on the unstrained sensor output. The locking mechanism is activated at $t = 12.5$ s.

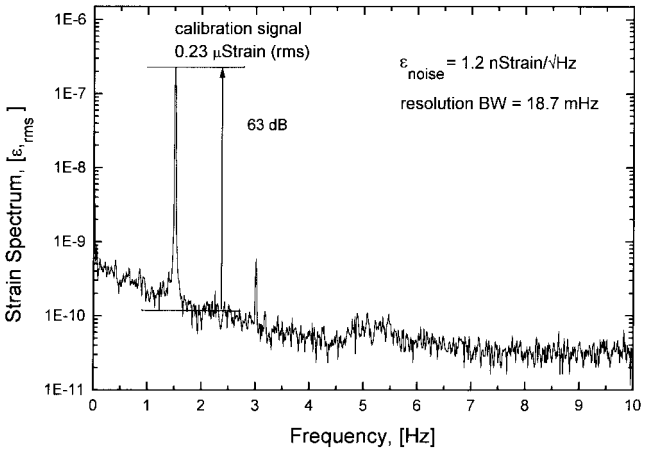

Fig. 5. Measured strain resolution spectrum in the low-frequency ("static") range. A calibration signal of 0.23 microstrain rms was applied at 1.5 Hz.

Locking the laser frequency to atomic lines has the advantage of practically eliminating the laser drifts, hence false strain signals which might be generated by such drifts are eliminated as well. To illustrate this, we have applied a triangular-shaped signal to the frequency modulation input of the laser, see Fig. 6. The reflection signal from the FBG followed these frequency changes, although the strain in the fiber was not altered. However, when the locking circuit was turned on and after a short transient, it canceled the effect of the triangular-shaped signal, and the laser frequency was kept locked. This is evident from the absorption signal trace, which remains at the minimum transmission level. Thus, the second harmonic frequency of the laser was fixed at the frequency of the highest absorption of the potassium transition. In this case, the FBG reflection signal remained at a fixed level, as it should.

The frequency variations of the interrogating laser, when locked to a Doppler-broadened atomic or molecular lines, having linewidths in the range from 300 to 1000 MHz, are typically in the 1 MHz range [11], which will be translated by the FBG sensor to an error of six nanostrain. This level is probably sufficient for most applications, but if higher performance is required, by using saturation spectroscopy techniques the laser may be locked to sub-Doppler lines, having typical linewidths in the range from 1 to 10 MHz. In this case, laser frequency stability in the kHz range can be achieved [23], and the respective strain error can be reduced to the picostrain level. The theoretical limitations imposed by laser noise on the strain sensitivity and dynamic range, derived in Section II, are also relevant to this type of sensor. Hence, the improved frequency stability when locked to sub-Doppler lines could also lead to higher strain sensitivity in sensors whose noise is dominated by the laser frequency noise. However, in our experiment, the low frequency noise was mainly caused by environmental surroundings.

The static strain sensitivity and error we have obtained are already comparable with the best-reported results of fiber-based strain sensors. For example Kersey *et al.* [2] reported resolution of 6 nanostrain/$\sqrt{\text{Hz}}$ and drift of 0.5 microstrain/h by using interferometric wavelength shift detection read-out and an isolated reference FBG. As for fiber sensors that are not based on FBG, two fiber etalon cavities were recently used for strain measurements with a sensitivity of 1.5 nanostrain rms [24].

IV. Summary

In summary, we have demonstrated a narrow-band interrogation technique for static FBG-based strain sensing. Static strain measurements were obtained by locking the laser frequency to an atomic line of potassium. The measured sensitivity of 1.2 nanostrain/$\sqrt{\text{Hz}}$ was limited by the environmental noise and the estimated error, assuming 1 MHz frequency stability is 6 nanostrain. We have verified that this method indeed canceled the frequency drifts of the laser by injecting a triangle wave to the PZT frequency actuator of the laser. Whereas in the free-running case, this led to variations in the reflected power from the FBG, which might be interpreted as a false strain signal, the reflected power remained constant when the laser was locked to the potassium line. The current sensor configuration may be also suitable

for measuring dynamic signals, although the operating point will now differ, in general, from the midreflection wavelength of the FBG. In this case, the maximum measurable dynamic strain is smaller than $\Delta\nu_{\max}/2$. Fortunately, the dynamic range can be further extended by using an FBG with a moderate reflection slope [9], [20], [21]. Experimentally, such dynamic measurements resulted in sensitivities of the same order as those of the configuration where the laser was locked to the midreflection point of the FBG [7].

Possible improvements in sensitivity and strain error can be achieved by locking the laser frequency to narrower sub-Doppler line. This method can be also used with other absorbers in addition to potassium. In particular, molecular lines [10] having a rich spectrum with many absorption lines, could enable multiplexed sensing by using a set of FBG's whose reflection frequencies match these absorption lines.

ACKNOWLEDGMENT

The authors would like to thank M. A. Arbore and M. M. Fejer for providing the waveguide frequency doubler. They also thank the reviewer of this paper for his helpful comments.

REFERENCES

[1] A. D. Kersey, M. A. Davis, H. J. Patrick, M. LeBlanc, K. P. Koo, C. J. Askins, M. A. Putnam, and E. J. Friebele, "Fiber grating sensors," *J. Lightwave Technol.*, vol. 15, pp. 1442–1463, 1997.

[2] A. D. Kersey, T. A. Berkoff, and W. W. Morey, "Fiber-optic Bragg gratin strain sensor with drift-compensated high resolution interferometric wavelength-shift detection," *Opt. Lett.*, vol. 18, pp. 72–74, 1993.

[3] ———, "High resolution fiber-grating based strain sensor with interferometric wavelength-shift detection," *Electron. Lett.*, vol. 28, pp. 236–238, 1992.

[4] K. P. Koo and A. D. Kersey, "Bragg grating-based laser sensors systems with interferometric interrogation and wavelength division multiplexing," *J. Lightwave Technol.*, vol. 13, pp. 1243–1249, 1995.

[5] M. LeBlanc, A. D. Kersey, and T. Tsai, "Sub-nanostrain strain measurements using a pi-phase shifted grating," in *Proc. 12 Int. Conf. Optic. Fiber Sensors OFS '97*, Williamsburg VA, 1967, pp. 28–30.

[6] H. Furuta and M. Ohtsu, "Evaluations of frequency shift and stability in rubidium vapor stabilized semiconductor laser," *Appl. Opt.*, vol. 28, pp. 3737–3743, 1989.

[7] B. Lissak, A. Arie, and M. Tur, "Highly sensitive dynamic strain measurements by locking lasers to fiber-Bragg gratings," *Opt. Lett.*, vol. 23, pp. 1930–1932, 1998.

[8] C. Miller, T. Li, J. Miller, F. Bao, and K. Hsu, "Multiplexed fiber gratings enhance mechanical sensing," *Laser Focus World*, 1998, pp. 119–123.

[9] See for example Innovative Fibers, 45 De Villebois, Suite 200, Gatineau (Quebec) Canada J8T 8J7.

[10] T. Ikegami, S. Sudo, and Y. Sakai, *Frequency Stabilization of Semiconductor Laser Diodes*. Boston, MA: Artech House, 1995.

[11] Y. C. Chung, "Frequency-locked 1.3 and 1.5 μm semiconductor lasers for lightwave systems applications," *J. Lightwave. Technol.*, vol. 8, pp. 869–876, 1990.

[12] M. Breton, P. Tremblay, C. Julien, N. Cyr, M. Tetu, and C. Latrasse, "Optically-pumped rubidium as a frequency standard at 196 THz," *IEEE Trans. Instrum. Measurement*, vol. 44, pp. 162–165 1995.

[13] M. Ohtsu and E. Ikegami, "Frequency stabilization of 1.5 μm DFB laser using internal second harmonic generation and atomic ^{87}Rb line," *Electron. Lett.*, vol. 25, pp. 22–23, 1989.

[14] V. Mahal, A. Arie, M. A. Arbore, and M. M. Fejer, "Quasiphase-matched frequency doubling in a waveguide of a 1560 nm diode laser and locking to the rubidium D_2 absorption lines," *Opt. Lett.*, vol. 21, pp. 1217–1219, 1996.

[15] W. Wang, A. M. Akulshin, and M. Ohtsu, "Pump-probe spectroscopy in potassium using an AlGaAs laser and the second harmonic generation of an InGaAsP laser for frequency stabilization and linking," *IEEE Photon. Technol. Lett.*, vol. 6, pp. 95–97, 1994.

[16] A. Bruner, A. Arie, M. A. Arbore, and M. M. Fejer, "Frequency stabilization of a diode laser at 1540 nm by locking to sub-Doppler lines of potassium at 770 nm," *Appl. Opt.*, vol. 37, pp. 1049–1052, 1998.

[17] D. S. Elliot, R. Roy, and S. J. Smith, "Extracavity laser band-shape and bandwidth modification," *Phys. Rev. A.*, vol. 26, pp. 12–18, 1982.

[18] B. Moslehi, "Noise power spectra of optical two-beam interferometers induced by the laser phase noise," *J. Lightwave Technol.*, vol. LT-4, pp. 1704–1710, 1986.

[19] S. Knudsen, A. B. Tveten, and A. Dandridge, "Measurements of fundamental thermal induced phase fluctuations in the fiber of a Sagnac interferometer," *IEEE Photon. Technol. Lett.*, vol. 7, pp. 90–92, 1995.

[20] A. D. Kersey, M. A. Davis, and T. Tsai, "Fiber optic Bragg grating strain sensor with direct reflectometric interrogation," in *Proc. 11 Int. Conf. Optic. Fiber Sensors OFS '96*, Sapporo, Japan, 1996, pp. 634–637.

[21] K. Sudgen, I. Bennion, A. Molony, and N. J. Copner, "Chirped gratings produced in photosensitive optical fibers by fiber deformation during exposure," *Electron. Lett.*, vol. 30, pp. 440–442, 1994.

[22] M. A. Arbore and M. M. Fejer, "Singly resonant optical parametric oscillation in periodically poled lithium niobate waveguides," *Opt. Lett.*, vol. 22, pp. 151–153, 1997.

[23] A. Bruner, V. Mahal, I. Kiryuschev, A. Arie, M. A. Arbore, and M. M. Fejer, "Frequency stability at the kilohertz level of a rubidium-locked diode laser at 192.114 THz," *Appl. Opt.*, vol. 37, pp. 6410–6414, 1998.

[24] E. J. Friebele, M. A. Putnam, H. J. Patric, A. D. Kersey, A. S. Greenblatt, G. P. Ruthven, M. H. Krim, and K. S. Gottschalck, "Ultrahigh sensitivity fiber-optic strain and temperature sensor," *Opt. Lett.*, vol. 23, pp. 222–224, 1998.

Ady Arie (M'96–SM'99) was born in Tel-Aviv, Israel, in 1963. He received the B.Sc. degree in physics and mathematics from the Hebrew University, Jerusalem, Israel, in 1983 and the M.Sc. degree in physics and Ph.D. degree in engineering from Tel-Aviv University, Tel-Aviv, Israel, in 1986 and 1992, respectively. His M.Sc. work was on light transmission through a modified cladding optical fiber and its application in sending. His Ph.D. dissertation work was on the effect of laser phase noise on fiber-optic sensing and signal processing devices.

From 1991 to 1993, he was a Fulbright and Wolfson Postdoctoral Scholar at the Byer Group, Edward L. Ginzton Lab, Stanford University, Stanford CA, where he developed frequency-stabilized Nd:YAG lasers and performed high-resolution spectroscopy of molecular iodine. In 1993, he joined the Faculty of Engineering of Tel-Aviv University, where he is a Senior Lecturer at the Department of Electrical Engineering-Physical Electronics. His current research interests include nonlinear optics in patterned nonlinear crystals, frequency stabilization of lasers in the 1.55 μm range, high-sensitvity laser spectroscopy, and precision optical measurements.

Dr. Arie is a member of the Optical Society of America (OSA).

Boaz Lissak was born in Tel-Aviv, Israel, in 1960. He received the B.S.E.E. and M.Sc. degrees in electrical engineering from Tel-Aviv University, Tel-Aviv, Israel, in 1985 and 1990, respectively. He is currently working towards the Ph.D degree in the Department of Interdisciplinary studies at the Faculty of Engineering, Tel-Aviv University.

Until 1995, he was with Optomic Lasers Ltd., where he was engaged in the design and development of an RF-excited CO_2 industrial laser for metal cutting and in Optomedic Medical Technologies Ltd., where a compact portable CO_2 medical laser was developed. His primary research interests includes fiber Bragg gratings and their applications in fiber sensors and fiber lasers.

Moshe Tur (M'87–SM'94–F'98) received the B.Sc. degree in mathematics and physics, from the Hebrew University, Jerusalem, Israel, in 1969 and the M.Sc. degree in applied physics from the Weizmann Institute of Science, Rehovot, Israel, in 1972, where he investigated electromagnetic wave propagation in cholesteric liquid crystals. After spending five years in the Israeli Defense Forces, he attended the Faculty of Engineering of Tel-Aviv University, Tel-Aviv, Israel, and received the Ph.D. degree in 1981.

His research there involved analytical, numerical and experimental investigations of wave propagation through random media, as well as fiber-optic communication systems. During the academic years 1981–1983, he was a Postdoctoral fellow (1981–1982) and then a Research Associate (1982–1983) at the Information System Laboratory and the Edward L. Ginzton Laboratory of Stanford University, Stanford, CA. At the Information System Laboratory, he studied speckle phenomena, various theories of wave propagation in random media, and asymptotic solutions of the fourth moment equation. At the Ginzton Laboratory, he participated in the development of new architectures for single-mode fiber-optic signal processing and investigated the effect of laser phase noise on such processors. He is presently a Professor of Electrical Engineering and Chairman of the Department of Interdisciplinary Studies in the Faculty of Engineering at Tel-Aviv University, Tel-Aviv, Israel, where he established a fiber-optic sensing laboratory. He has authored or coauthored more than 150 journal and conference technical papers with recent emphasis on fiber-optic bit rate limiters, fiber lasers, fiber-optic sensor arrays, the statistics of phase-induced intensity noise in fiber-optic systems, fiber sensing in smart structures, fiber Bragg gratings, polarization mode dispersion, and advanced fiber-optic communication systems.

Dr. Tur is a Fellow of the Optical Society of America (OSA).